Germline stem cells and follicular renewal in the postnatal mammalian ovary

Joshua Johnson*, Jacqueline Canning*, Tomoko Kaneko, James K. Pru & Jonathan L. Tilly

Vincent Center for Reproductive Biology, Vincent Obstetrics and Gynecology Service, Massachusetts General Hospital, and Department of Obstetrics, Gynecology and Reproductive Biology, Harvard Medical School, Boston, Massachusetts 02114, USA

* These authors contributed equally to this work

A basic doctrine of reproductive biology is that most mammalian females lose the capacity for germ-cell renewal during fetal life, such that a fixed reserve of germ cells (oocytes) enclosed within follicles is endowed at birth. Here we show that juvenile and adult mouse ovaries possess mitotically active germ cells that, based on rates of oocyte degeneration (atresia) and clearance, are needed to continuously replenish the follicle pool. Consistent with this, treatment of prepubertal female mice with the mitotic germ-cell toxicant busulphan eliminates the primordial follicle reserve by early adulthood without inducing atresia. Furthermore, we demonstrate cells expressing the meiotic entry marker synaptonemal complex protein 3 in juvenile and adult mouse ovaries. Wild-type ovaries grafted into transgenic female mice with ubiquitous expression of green fluorescent protein (GFP) become infiltrated with GFP-positive germ cells that form follicles. Collectively, these data establish the existence of proliferative germ cells that sustain oocyte and follicle production in the postnatal mammalian ovary.

Although males retain germline stem cells (GSCs) for spermatogenesis throughout adult life, oocyte production in females of most mammalian species is believed to cease before birth[1–5]. Accordingly, a central dogma of mammalian reproductive biology is that females are born with a finite, non-renewing pool of germ cells, all of which are arrested in meiosis I (oocytes) and are enclosed by somatic cells in structures referred to as follicles[1–5]. Oocyte numbers decline throughout postnatal life[6–8] through mechanisms involving apoptosis[9,10], eventually leaving the ovaries barren of germ cells[11]. In humans, exhaustion of the oocyte reserve occurs around the fifth decade of life, driving the menopause[12]. The process that is believed to occur in female mammals with respect to germ-cell development differs from that of several invertebrate organisms, including *Drosophila melanogaster*, in which GSCs maintain oocyte production in adult ovaries[13–15]. This apparent evolutionary disparity is female-specific, as the role of GSCs in maintaining spermatogenesis has been documented in essentially all metazoan species[13–15].

Discordance in follicle loss versus atresia

To better define germ-cell dynamics in female mammals, a study was initially undertaken to assess the numbers of healthy (non-atretic) and degenerating (atretic) follicles in ovaries of C57BL/6 mice. Analysis of non-atretic quiescent (primordial) and early growing (primary, preantral) follicle numbers revealed that approximately one-third of the peak endowment of immature follicles was lost during development to young adulthood (Fig. 1a), consistent with past studies of follicle depletion in mice[7]. However, unlike all previous studies of follicle development in mammals that we are aware of, a parallel assessment of immature follicle atresia was conducted and compared with the numbers of non-atretic follicles lost over time. Through the first 20 days of age, atresia occurred at a low but constant rate (Fig. 1b), consistent with a proportional decline in non-atretic follicle numbers during this time period (Fig. 1a). However, the incidence of atresia increased markedly by day 30 and further by day 40, reaching a peak level of more than 1,200 dying follicles per ovary on day 42 that was maintained well into reproductive life (Fig. 1b).

Clearance of apoptotic cells *in vivo* occurs within 3–18 h[16–18]. Nonetheless, experiments were conducted to rule out the possibility that the large atretic follicle population observed in adult animals simply represented accumulation of oocyte corpses in follicles that had degenerated weeks earlier. The first experiment, based on past studies showing that extensive levels of oocyte apoptosis occur in the newborn mouse ovary coincident with follicle formation[19,20], evaluated changes in the number of non-atretic oocytes between days 1 and 4 postpartum compared with the number of degenerative oocytes on day 4. More than 8,000 non-atretic oocytes were present per ovary on day 1, and this pool was reduced by almost 50% by day 4 (Supplementary Table S1). However, only 218 degenerative oocytes per ovary were found on day 4, indicating that over 3,300 oocytes had died and been cleared from the ovary between days 1 and 4 postpartum (Supplementary Table S1). The second approach to assess clearance rates of degenerative oocytes used the chemical 9,10-dimethylbenz[*a*]anthracene (DMBA) to synchronize primordial and primary follicle atresia. Past studies have shown that DMBA induces degeneration of immature oocytes in a manner that morphologically resembles developmental oocyte death[21]. In addition, the pro-apoptotic Bax protein is required for immature follicle atresia under normal conditions[9] and in response to DMBA exposure[22], further underscoring the similarities between the two processes. In female mice given a single injection of DMBA, the incidence of follicle atresia increased markedly between 24 and 48 h after injection, and remained at a plateau of approximately 850 atretic follicles per ovary from 48 to 72 h after injection (Fig. 1c). By 96 h after injection, there were no healthy primordial or primary follicles remaining in the ovaries, and the incidence of atresia returned to near-basal levels (Fig. 1c). Therefore, similar to the clearance rate of degenerative oocytes between postnatal days 1 and 4 discussed earlier, DMBA-induced synchronization of atresia revealed that over 3,500 oocytes contained within primordial and primary follicles initiated apoptosis and were cleared from the ovary within a 3-day period.

Given this, the finding that from 1% (days 8, 12 and 20) to as much as 16% (day 40) or more (33%, day 42; Fig. 1d) of the

immature follicle pool is degenerating at any given time under normal conditions would be predictive of complete exhaustion of the follicle reserve by young adulthood. However, the non-atretic pool of follicles declined from peak levels on day 12 by only 36% on day 40 (Fig. 1a). This indicated that the rate of follicle depletion during postnatal life, as determined by assessing changes in non-atretic follicle numbers, was highly incongruous with the numbers of follicles actually being eliminated from the ovaries through atresia in the same time frame. To confirm that these findings were not a phenomenon related to C57BL/6 mice, changes in follicle numbers from birth to adulthood were analysed in other strains of mice, and compared with corresponding data from C57BL/6 females. In CD1 mice, the non-atretic follicle pool declined by only 4% between days 4 and 42 postpartum, despite a relatively high incidence of atresia, comparable to that observed in C57BL/6 females (Fig. 1d). Even more striking, the non-atretic follicle population in AKR/J mice was 20% larger on day 42 than on day 4, again despite a marked incidence of atresia (Fig. 1d). These data, which extend past work showing that genetic strain has a marked impact on female germ-cell dynamics[23], highlight a clear discordance between changes in non-atretic follicle numbers and the corresponding incidence of atresia in the postnatal mammalian ovary.

Postnatal female germ-cell proliferation

In the light of these data, the possibility that oocyte and follicle renewal are still ongoing in the postnatal mouse ovary was examined by several approaches. First, histological analysis of juvenile and young adult ovaries revealed the presence of large ovoid cells, resembling germ cells of fetal mouse ovaries[24,25], in the surface epithelial cell layer covering the ovary (Fig. 2a). However, these cells were not intimately associated with smaller squamous epithelial cells in any type of structure reminiscent of a follicle. Immunohistochemical staining for mouse Vasa homologue (MVH), a gene expressed exclusively in germ cells of both vertebrate and invertebrate species[26,27], confirmed that these large ovoid cells were of a germline lineage (Fig. 2b). To document the proliferative potential of these MVH-positive cells, juvenile and young adult female mice were injected with 5-bromodeoxyuridine (BrdU) and ovaries were collected 1 h later for dual immunostaining analysis of BrdU incorporation and MVH expression. These experiments confirmed the presence of BrdU–MVH double-positive cells, all of which were found in the ovarian surface epithelium (Fig. 2d–f). This finding was not the result of BrdU incorporation associated with mitochondrial DNA replication or DNA repair in post-meiotic female germ cells, as the degree of BrdU incorporation observed in cells due to either of these processes is several log orders less than that seen during replication of the nuclear genome during mitosis[28,29]. Consistent with this, the BrdU immunoreaction in MVH-positive cells was comparable in intensity to that observed in replicating follicular somatic (granulosa) cells, and, more importantly, was never observed in adjacent oocytes contained within follicles (Fig. 2d, e). Analysis of ovaries immunostained for MVH and counterstained with propidium iodide confirmed the presence of germ cells in various stages of mitosis (Fig. 2g, h). These data, taken with the histomorphometric findings discussed earlier, build a strong case for germ-cell proliferation and follicle renewal in the postnatal mouse ovary.

Meiotic entry in postnatal ovaries

Replication of germ cells to produce oocytes for follicle formation in postnatal life would require expression of genes involved in the initiation of meiosis. Thus, expression of synaptonemal complex protein 3 (SCP3), a meiosis-specific protein needed for formation of axial lateral elements of the synaptonemal complex[30,31], was examined in juvenile and young adult mouse ovaries. Immunohistochemical localization of SCP3 revealed individual immunoreactive cells in or proximal to the surface of the ovary (Fig. 3a, b). The possibility that SCP3 was simply carried over as a stable protein product in oocytes formed during the perinatal period was ruled out by the finding that oocytes contained within immature follicles were not immunoreactive (Fig. 3c, d). Postnatal ovarian expression

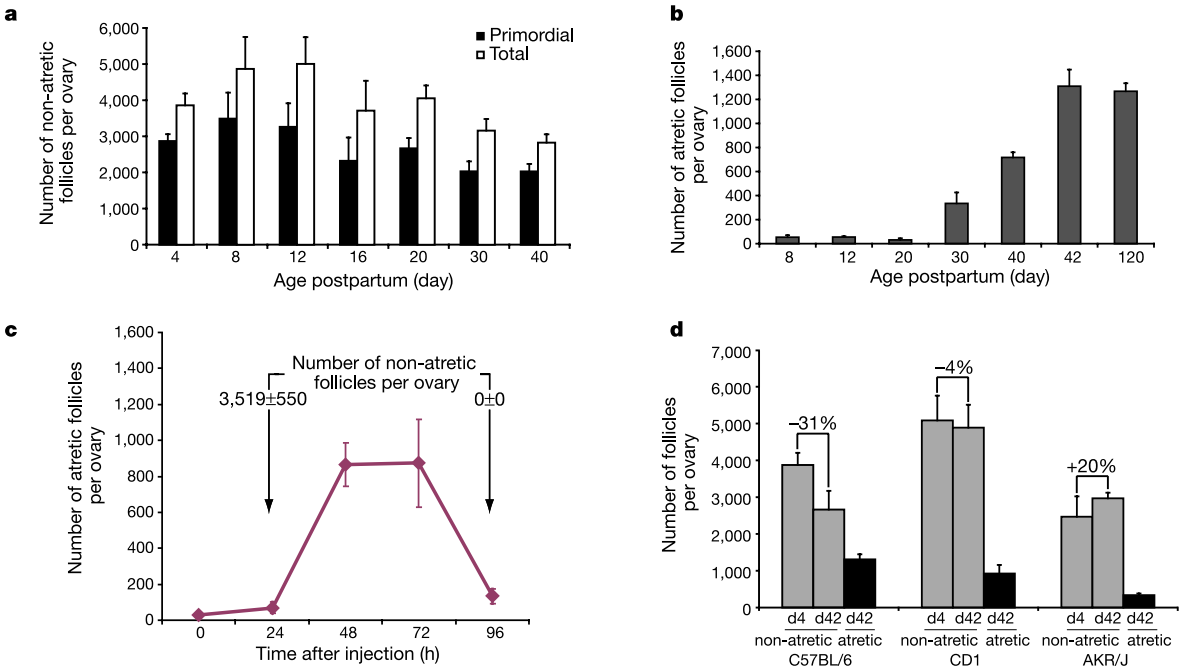

Figure 1 Postnatal ovarian germ-cell dynamics. **a**, **b**, Numbers of non-atretic (**a**) and atretic (**b**) primordial and total immature (primordial, primary, small preantral) follicles in mouse ovaries during postnatal development (**b**, total immature follicles; mean ± standard error, $n = 3$–4 mice per age group). **c**, Incidence of primordial and primary follicle atresia in ovaries exposed to DMBA on day 25 postpartum (mean ± standard error, $n = 4$–5 mice per time point). **d**, Comparison of non-atretic and atretic immature follicle numbers in C57BL/6, CD1 and AKR/J strains of mice (mean ± standard error, $n = 3$–5 mice per age group).

of *Scp3* was confirmed at the messenger RNA level, as was expression of the endonuclease *Spo11* and the recombinase *Dmc1* (Fig. 3e), both of which are also required for the initiation of meiosis in mammals[32]. Past work has shown that expression of *Scp3* and *Dmc1* in germ cells is restricted to the zygotene or pachytene stages of meiosis[30–32]. As these stages are earlier than the late diplotene stage where the first meiotic arrest in oocytes is observed[33], the presence of these mRNA transcripts, like SCP3 protein, cannot be considered simply as a reflection of oocytes being in meiosis. The levels of *Scp3*, *Spo11* and *Dmc1* expression in adult ovaries ranged from 6% (*Spo11*, *Dmc1*) to 25% (*Scp3*) of those observed in adult testes (Fig. 3f), which is significant considering that daily postnatal germ-cell output in the testis far exceeds that estimated for the ovaries (see next section). Ovarian expression of all three meiosis-related genes declined with age (Fig. 3e), and minimal to no expression of these genes was observed in non-gonadal tissues (Fig. 3g).

Primordial follicle renewal

The importance of proliferative germ cells to replenishment of the postnatal follicle pool was further verified by the use of busulphan, a germ-cell toxicant widely used in spermatogonial stem-cell characterization in male mice[34–36]. In the testis, busulphan specifically targets GSCs and spermatogonia, but not post-meiotic germ cells, leading to spermatogenic failure[34]. Female rodents exposed *in utero* show a similar gametogenic failure in response to busulphan only if the chemical is given during the window of fetal ovarian germ-cell proliferation, as females exposed to busulphan *in utero* after germ-cell proliferation has ceased are born with ovaries that are histologically and functionally similar to ovaries of vehicle-exposed mice[37]. In the present experiments, female mice were injected with vehicle or busulphan on day 25 and again on day 35, and ovaries were collected 10 days after the second injection to analyse changes in non-atretic primordial follicle numbers. Ovaries of females treated with busulphan possessed less than 5% of the primordial follicle pool present in vehicle-treated controls 20 days after the start of the experiment (Fig. 4a). However, busulphan-exposed ovaries retained an otherwise normal histological appearance, including the presence of healthy maturing follicles with non-degenerative oocytes, as well as corpora lutea, indicative of ovulation (Fig. 4b–e).

A previous investigation of adult female mice exposed to busulphan reported a similar decline in immature follicle numbers with complete oocyte loss occurring sometime between 2–17 weeks after injection[38]. The depletion of follicles was attributed to cytotoxic actions of busulphan in follicle-enclosed oocytes, although the incidence of atresia was not directly evaluated[38]. If busulphan causes ovarian failure in adult mice because of toxicity to existing oocytes, we found it puzzling that the time frame for oocyte loss after this insult would be weeks to months rather than hours to days, as is the case with other germ-cell toxicants such as DMBA (Fig. 1c) or cyclophosphamide[39]. To clarify whether loss of primordial follicles observed in busulphan-treated females (Fig. 4a) results from toxicity to existing oocytes, ovaries were collected from female mice at multiple points during and after the busulphan dosing regimen described above, and they were analysed for the incidence of primordial follicle atresia. Busulphan caused a slight, transient increase in the number of atretic primordial follicles, with a plateau of only 46 per ovary 5 days after the first injection that quickly declined to basal levels thereafter (Fig. 4a, inset). This relatively minor and acute atretic response to busulphan was negligible considering that over 2,000 primordial follicles were absent in busulphan-exposed ovaries compared with vehicle-treated controls

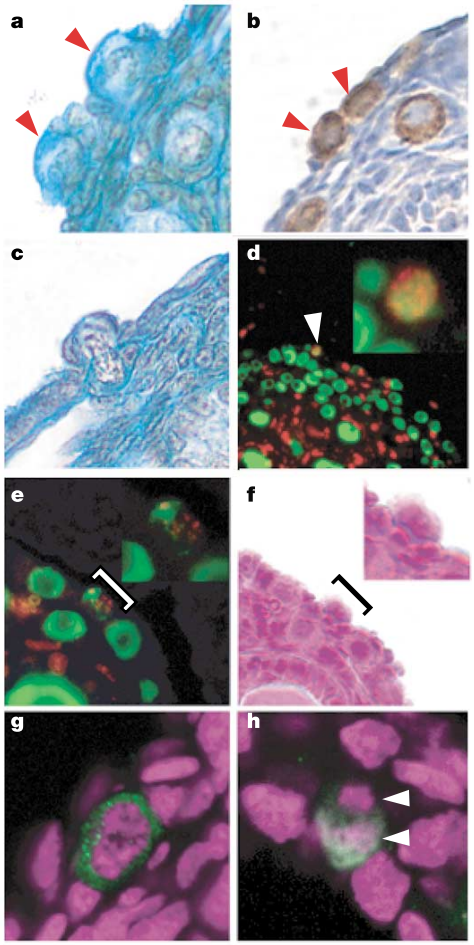

Figure 2 Germ-cell proliferation in juvenile and young adult ovaries. **a**, Presumptive GSCs (arrowheads) in the surface epithelium. **b**, Immunohistochemical detection of MVH (brown reaction product) in presumptive GSCs (arrowheads). **c**, Presumptive GSC undergoing mitosis across the surface epithelium. **d**, **e**, Dual immunostaining for BrdU (red) and MVH (green) in juvenile and young adult mouse ovaries. **f**, Haematoxylin and eosin staining of the section shown in **e**, highlighting the dividing germ cell. **g**, **h**, Chromatin morphology (propidium iodide counterstaining, violet) within MVH-positive cells (green) shows a germ cell in prometaphase (**g**) and a germ cell in metaphase (**h**; sister chromatids highlighted by arrowheads).

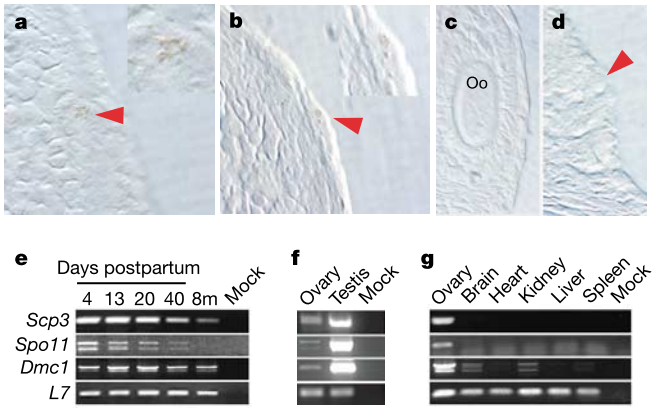

Figure 3 Meiotic entry gene expression in postnatal ovaries. **a**–**d**, SCP3 immunostaining (brown) in single cells (**a**, **b**) located in or proximal to the surface epithelium of juvenile and young adult mouse ovaries (**c**, small preantral follicle; **d**, primordial follicle with oocyte marked by arrowhead). Oo, oocyte. **e**, Expression of *Scp3*, *Spo11* and *Dmc1* in ovaries collected at the indicated days of age or at 8 months (8 m) postpartum. *L7*, ribosomal gene co-amplified as an internal control; mock, mock-transcribed ovarian RNA samples. **f**, **g**, *Scp3*, *Spo11* and *Dmc1* expression in ovaries versus testes (**f**) or in various tissues (**g**) collected from young adult mice.

(Fig. 4a). These data reinforce the concept that proliferative germ cells not only persist in the postnatal ovary but also are required to routinely renew the follicle pool.

To determine the rate of primordial follicle renewal in the postnatal mouse ovary, we evaluated our findings in the context of a past investigation of the kinetics of follicle maturation in female mice[7]. Faddy and colleagues[7] demonstrated that the primordial follicle pool is decreased on average by 89 follicles per day, owing to either degeneration or growth activation to the primary stage of development, between days 14 and 42 postpartum. In our study's comparable window of time (day 16–40 postpartum; Fig. 1a), this rate of exit would be expected to reduce the primordial follicle population by 2,136 follicles over this 24-day period. However, the number of primordial follicles declined by only 294 between days 16 and 40 postpartum (Fig. 1a). The difference between these two values—or 1,842 primordial follicles—represents the rate of primordial follicle renewal over this 24-day period, yielding an average of 77 new primordial follicles per ovary per day. If this calculation is accurate, then the rate of primordial follicle depletion per day should be the difference between the rate of exit per day provided by Faddy and co-workers[7] (89 follicles) and the rate of renewal per day (77 follicles), for a net loss of 12 primordial follicles per ovary per day. Using this value, the primordial follicle pool would be expected to decline between days 16 and 40 postpartum by a total of 288 follicles, a number very close to that derived from comparing the actual counts of non-atretic primordial follicles on day 16 versus day 40 (2,334 versus 2,040, or a net loss of 294 primordial follicles; Fig. 1a).

Folliculogenesis and germline stem cells

In a final set of experiments, transgenic mice with ubiquitous expression of GFP[40] were used to provide additional evidence for ongoing folliculogenesis in postnatal life. Ovarian fragments harvested from adult wild-type mice were grafted into the ovarian bursal cavity of transgenic female siblings after removal of approximately one-half of the host's ovary. After 3–4 weeks, ovaries were collected and processed for GFP expression. The grafted ovarian fragments, upon gross visual inspection, showed evidence of neovascularization and adhesion to the host ovarian tissue (Supplementary Fig. S1). Confocal microscopic analysis revealed

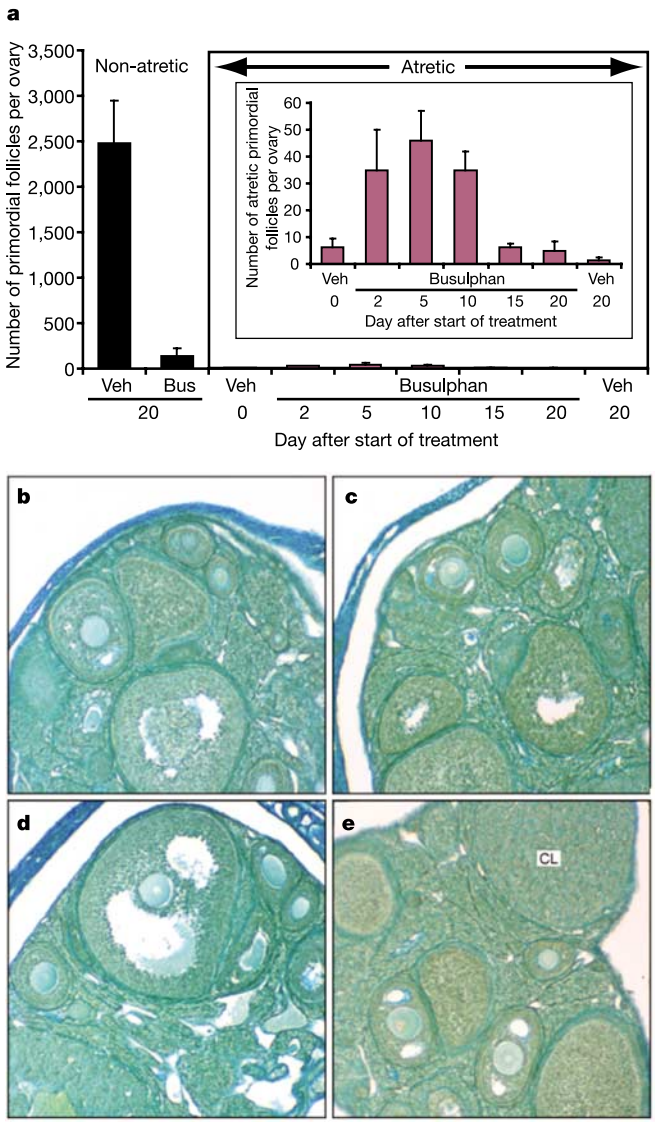

Figure 4 Busulphan eliminates the primordial follicle reserve in adult female mice. **a**, Numbers of non-atretic and atretic primordial follicles present in the ovaries of vehicle (Veh)- or busulphan (Bus)-treated mice (mean ± standard error, $n = 3$–4 mice per data point). The inset shows results for primordial follicle atresia. **b**–**e**, Histological appearance of ovaries of vehicle-treated (**b**) or busulphan-treated (**c**–**e**) mice, underscoring the lack of nonspecific or widespread cytotoxic effects of busulphan on the ovaries or existing oocytes within developing follicles. Note also the presence of corpora lutea (CL) in busulphan-exposed ovaries (**e**), indicative of normal ovulatory function in these animals.

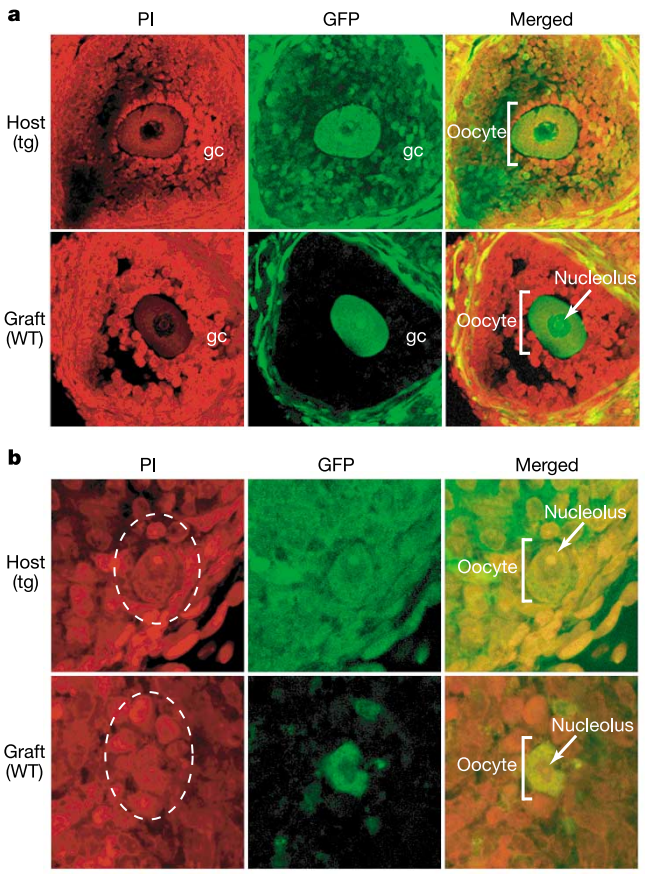

Figure 5 GFP-transgenic germ cells form follicles in wild-type ovaries. **a**, **b**, GFP expression (green) in sections of host (GFP-transgenic, tg) and grafted (wild type, WT) ovarian tissues counterstained with propidium iodide (PI; red). **a**, Antral follicle in grafted ovarian tissue containing a GFP-positive oocyte enclosed within GFP-negative granulosa cells (gc). A maturing antral follicle in the host ovary is shown for comparison. **b**, Primary follicle in grafted ovarian tissue containing a GFP-positive oocyte enclosed within GFP-negative granulosa cells (broken white line). A primary follicle in the host ovary is shown for comparison. Additional examples and details are provided in the Supplementary Information.

follicle-enclosed, GFP-positive oocytes in the wild-type ovarian fragments that were indistinguishable from follicle-enclosed oocytes in the host ovarian tissue (Fig. 5; see also Supplementary Fig. S3). Moreover, the granulosa cells enveloping the GFP-positive oocytes in the grafts were negative for GFP, indicating that transgenic germ cells had infiltrated the grafted tissue and initiated folliculogenesis with the resident wild-type somatic cells.

This latter finding, when considered with results from past studies of mammalian stem-cell migration to their natural niches after introduction into a host[41–44], suggests that GSCs exist in the postnatal mouse ovary. In the testis and in the *Drosophila* ovary, GSCs are defined by their capacity to self-renew after division while simultaneously producing a daughter cell capable of differentiating into a mature egg or sperm—a process referred to as asymmetric division[13–15]. To sustain the addition of new primordial follicles during juvenile and adult life, the mouse ovary must possess either a small pool of asymmetrically dividing GSCs or a large pool of non-renewing, pre-meiotic germ cells that produce oocytes after symmetric divisions. Given that histological surveys did not reveal any evidence in support of the latter possibility (data not shown), the large ovoid germ cells in the surface epithelium (Fig. 2a, b) were then considered as candidates for GSCs. Histomorphometric studies at day 30 postpartum revealed the presence of 63 ± 8 such cells per ovary (mean $\pm$ standard error, $n = 4$ mice), a number close to that expected for a small pool of asymmetrically dividing germ cells.

Discussion

In 1921, Pearl and Schoppe cited a "basic biological doctrine that during the life of the individual there neither is nor can be any increase in the number of primary oocytes beyond those originally laid down when the ovary was formed"[45]. This concept was solidified as dogma in 1951 in a paper that critically evaluated, and effectively dispelled, any work contrary to the belief that mammalian females are endowed with a finite and non-renewing germ-cell reserve during the perinatal period[1]. Although this dogma has persisted for more than 50 yr, the present study provides evidence that challenges the validity of this belief, which represents one of the most basic underpinnings of reproductive biology. The data shown also underscore the significance of mammalian female GSCs to regenerating the follicle reserve in adult life. If one considers that the total pool of non-atretic immature follicles per ovary in C57BL/6 mice is less than 4,000 at puberty, the presence of between 700–1,300 atretic immature follicles at this time point, even with a 3-day clearance rate for their removal, would be predictive of complete exhaustion of the follicle reserve in a few weeks. However, C57BL/6 female mice possess primordial and early growing follicles past 12 months of age[11]. Therefore, in addition to providing new directions to explore with respect to elucidating the biology of mammalian female GSCs, this work has significant clinical implications related to therapeutic expansion of the follicle reserve as a means to postpone normal or premature ovarian failure. □

Methods

Animals

Age-specified or timed-pregnant wild-type C57BL/6 and CD1 female mice were purchased from Charles River Laboratories, whereas AKR/J mice were obtained from Jackson Laboratories. For the atresia synchronization and oocyte clearance experiments, C57BL/6 female mice were given a single intraperitoneal injection of vehicle (corn oil) or DMBA (80 mg per kg body weight; re-suspended in corn oil) on day 25 postpartum, and ovaries were collected just before injection and at 24 h intervals after injection for up to 96 h. For the busulphan experiments, C57BL/6 female mice were given an intraperitoneal injection of vehicle (DMSO) or busulphan (20 mg per kg body weight; re-suspended in DMSO) on day 25 and again on day 35 postpartum, and ovaries were collected at the indicated times for analysis. Transgenic mice with ubiquitous expression of GFP[40] were obtained from Jackson Laboratories (strain: STOCK TgN(GFPU)5Nagy) and used for ovarian grafting experiments as described below (see 'Ovarian grafting' section of Methods). All animal work was conducted using procedures reviewed and approved by the institutional animal care and use committee of Massachusetts General Hospital, and were conducted in accordance with the NIH Guide for the Care and Use of Laboratory Research Animals.

Ovarian histology and follicle counts

Ovaries were fixed (0.34 N glacial acetic acid, 10% formalin, 28% ethanol), paraffin embedded, serially sectioned (8 μm), aligned in order on glass microscope slides, and stained with haematoxylin and picric methyl blue. The number of non-atretic or atretic primordial, primary and preantral follicles was then determined, as described[9,46] (see Supplementary Information for additional details). Immature follicles were scored as atretic if the oocyte was degenerating (convoluted, condensed) or fragmented. Grossly atretic immature follicles lacking oocyte remnants were not included in the analyses.

Immunohistochemistry

After fixation in 4% neutral-buffered paraformaldehyde and embedding in paraffin, 6-μm tissue sections were cut from the ovaries and mounted on slides. The sections were de-waxed in xylenes, re-hydrated, and boiled for 5 min in 10 mM sodium citrate using a microwave. Primary antibodies specific for MVH[26], BrdU (Zymed), or SCP3 (refs 47, 48) were then used for immunohistochemical analyses as per the suppliers' recommendations (see Supplementary Information for details). To visualize chromatin morphology within MVH-positive cells, MVH detection in fixed ovarian tissue sections was performed, and the sections were then incubated in 10 μg ml^{-1} RNase A for a minimum of 2 h at 37 °C. After washing, the sections were mounted in the presence of 1.5 μg ml^{-1} propidium iodide (Vector Labs), as described[49], and visualized using a Zeiss LSM 5 Pascal confocal microscope. For SCP3 immunohistochemistry, photomicrographs of the sections were taken under Hoffman optics without prior counterstaining to prevent masking of the immunoreaction signal by vital dyes.

Reverse transcription PCR analysis

For ovaries collected at each time point and for control tissues, total RNA was extracted and 1 μg of total RNA was reverse transcribed (Superscript II RT; Invitrogen) using oligo-dT primers. Amplification via 28 cycles of PCR was performed using *Taq* polymerase and buffer D (Epicentre) with primer sets specific for each gene (Supplementary Table S2). The ribosomal gene *L7* was co-amplified and used as a loading control for each sample, and 28 cycles were found to be within the linear range of amplification for each experimental primer set (data not shown). All PCR products were isolated, subcloned and sequenced for confirmation. In those samples showing more than one amplified product per primer set, each band was isolated, subcloned and sequenced. These additional bands were determined to be known splice variants of the targeted genes (*Dmc-1*/*Dmc-1d*; *Spo11a*/*Spo11b*) (Supplementary Table S2).

Ovarian grafting

Heterozygous transgenic male and female mice with ubiquitous expression of GFP[40] were mated to generate wild-type and transgenic female offspring for intrabursal ovarian grafting. Briefly, young adult (58–69 days postpartum) transgenic female mice were anaesthetized (avertin, 200 mg per kg, intraperitoneal) to expose one of the two ovaries in each mouse through dorso-lateral incisions. For each animal, a small hole was cut in the ovarian bursa laterally near the hilus, and approximately one-half of the host ovary was removed in preparation for grafting. Ovaries collected from donor (wild-type littermate) female mice were bisected, and one-half of a wild-type ovary was placed within the transgenic recipient's bursal cavity in contact with the remaining host ovarian tissue. The reproductive tract was then allowed to settle back into the peritoneal cavity and the incision was closed. A total of six transgenic hosts were used for this experiment, four of which received unilateral wild-type ovarian grafts while the remaining two received bilateral wild-type ovarian grafts. Between 3–4 weeks after surgery, the ovarian tissues were removed and processed for GFP visualization, after propidium iodide counterstaining, by confocal laser scanning microscopy[50].

Received 11 September; accepted 23 December 2003; doi:10.1038/nature02316.

1. Zuckerman, S. The number of oocytes in the mature ovary. *Recent Prog. Horm. Res.* **6,** 63–108 (1951).
2. Borum, K. Oogenesis in the mouse. A study of meiotic prophase. *Exp. Cell Res.* **24,** 495–507 (1961).
3. Peters, H. Migration of gonocytes into the mammalian gonad and their differentiation. *Phil. Trans. R. Soc. Lond. B* **259,** 91–101 (1970).
4. McLaren, A. Meiosis and differentiation of mouse germ cells. *Symp. Soc. Exp. Biol.* **38,** 7–23 (1984).
5. Anderson, L. D. & Hirshfield, A. N. An overview of follicular development in the ovary: from embryo to the fertilized ovum *in vitro*. *Md Med. J.* **41,** 614–620 (1992).
6. Faddy, M. J., Jones, E. C. & Edwards, R. G. An analytical model for ovarian follicle dynamics. *J. Exp. Zool.* **197,** 173–186 (1976).
7. Faddy, M. J., Telfer, E. & Gosden, R. G. The kinetics of pre-antral follicle development in ovaries of CBA/Ca mice during the first 14 weeks of life. *Cell Tissue Kinet.* **20,** 551–560 (1987).
8. Faddy, M. J. Follicle dynamics during ovarian ageing. *Mol. Cell. Endocrinol.* **163,** 43–48 (2000).
9. Perez, G. I. *et al.* Prolongation of ovarian lifespan into advanced chronological age by *Bax*-deficiency. *Nature Genet.* **21,** 200–203 (1999).
10. Tilly, J. L. Commuting the death sentence: how oocytes strive to survive. *Nature Rev. Mol. Cell Biol.* **2,** 838–848 (2001).
11. Gosden, R. G., Laing, S. C., Felicio, L. S., Nelson, J. F. & Finch, C. E. Imminent oocyte exhaustion and reduced follicular recruitment mark the transition to acyclicity in aging C57BL/6J mice. *Biol. Reprod.* **28,** 255–260 (1983).
12. Richardson, S. J., Senikas, V. & Nelson, J. F. Follicular depletion during the menopausal transition: evidence for accelerated loss and ultimate exhaustion. *J. Clin. Endocrinol. Metab.* **65,** 1231–1237 (1987).
13. Lin, H. The tao of stem cells in the germline. *Annu. Rev. Genet.* **31,** 455–491 (1997).
14. Spradling, A. H., Drummond-Barbosa, D. & Kai, T. Stem cells find their niche. *Nature* **414,** 98–104 (2001).

15. Lin, H. The stem-cell niche theory: lessons from flies. *Nature Rev. Genet.* **3,** 931–940 (2002).
16. Wyllie, A. H., Kerr, J. F. R. & Currie, A. R. Cell death: the significance of apoptosis. *Int. Rev. Cytol.* **68,** 251–306 (1980).
17. Ijiri, K. & Potten, C. S. Response of intestinal cells of differing topographical and hierarchical status to ten cytotoxic drugs and five sources of radiation. *Br. J. Cancer* **47,** 175–185 (1983).
18. Bursch, W., Paffe, S., Putz, B., Barthel, G. & Schulte-Hermann, R. Determination of the length of the histological stages of apoptosis in normal liver and in altered hepatic foci of rats. *Carcinogenesis* **11,** 847–853 (1990).
19. Ratts, V. S., Flaws, J. A., Kolp, R., Sorenson, C. M. & Tilly, J. L. Ablation of *bcl-2* gene expression decreases the numbers of oocytes and primordial follicles established in the post-natal female mouse gonad. *Endocrinology* **136,** 3665–3668 (1995).
20. Pepling, M. E. & Spradling, A. C. Mouse ovarian germ cell cysts undergo programmed breakdown to form primordial follicles. *Dev. Biol.* **234,** 339–351 (2001).
21. Mattison, D. R. Morphology of oocyte and follicle destruction by polycyclic aromatic hydrocarbons in mice. *Toxicol. Appl. Pharmacol.* **53,** 249–259 (1980).
22. Matikainen, T. *et al.* Aromatic hydrocarbon receptor-driven *Bax* gene expression is required for premature ovarian failure caused by biohazardous environmental chemicals. *Nature Genet.* **28,** 355–360 (2001).
23. Canning, J., Takai, Y. & Tilly, J. L. Evidence for genetic modifiers of ovarian follicular endowment and development from studies of five inbred mouse strains. *Endocrinology* **144,** 9–12 (2003).
24. Crone, M., Levy, E. & Peters, H. The duration of the premeiotic DNA synthesis in mouse oocytes. *Exp. Cell Res.* **39,** 678–688 (1965).
25. Morita, Y. *et al.* Requirement for phosphatidylinositol-3′-kinase in cytokine-mediated germ cell survival during fetal oogenesis in the mouse. *Endocrinology* **140,** 941–949 (1999).
26. Fujiwara, Y. *et al.* Isolation of a DEAD-family protein gene that encodes a murine homolog of *Drosophila* vasa and its specific expression in germ cell lineage. *Proc. Natl Acad. Sci. USA* **91,** 12258–12262 (1994).
27. Noce, T., Okamoto-Ito, S. & Tsunekawa, N. Vasa homolog genes in mammalian germ cell development. *Cell Struct. Funct.* **26,** 131–136 (2001).
28. Selden, J. R. *et al.* Statistical confirmation that immunofluorescent detection of DNA repair in human fibroblasts by measurement of bromodeoxyuridine incorporation is stoichiometric and sensitive. *Cytometry* **14,** 154–167 (1993).
29. Davis, A. F. & Clayton, D. A. *In situ* localization of mitochondrial DNA replication in intact mammalian cells. *J. Cell Biol.* **135,** 883–893 (1996).
30. Yuan, L. *et al.* The murine *SCP3* gene is required for synaptonemal complex assembly, chromosome synapsis, and male fertility. *Mol. Cell* **5,** 73–83 (2000).
31. Yuan, L. *et al.* Female germ cell aneuploidy and embryo death in mice lacking the meiosis-specific protein SCP3. *Science* **296,** 1115–1118 (2002).
32. Cohen, P. & Pollard, J. W. Regulation of meiotic recombination and prophase I progression in mammals. *Bioessays* **23,** 996–1009 (2001).
33. Gosden, R., Clarke, H. & Miller, D. in *Reproductive Medicine—Molecular, Cellular and Genetic Fundamentals* (ed. Fauser, B. C. J. M.) 365–380 (Parthenon, New York, 2003).
34. Bucci, L. R. & Meistrich, M. L. Effects of busulfan on murine spermatogenesis: cytotoxicity, sterility, sperm abnormalities, and dominant lethal mutations. *Mutat. Res.* **176,** 259–268 (1987).
35. Brinster, R. L. & Zimmermann, J. W. Spermatogenesis following male germ-cell transplantation. *Proc. Natl Acad. Sci. USA* **91,** 11298–11302 (1994).
36. Brinster, C. J. *et al.* Restoration of fertility by germ cell transplantation requires effective recipient preparation. *Biol. Reprod.* **69,** 412–420 (2003).
37. Pelloux, M. C., Picon, R., Gangnerau, M. N. & Darmoul, D. Effects of busulphan on ovarian folliculogenesis, steroidogenesis and anti-Müllerian activity of rat neonates. *Acta Endocrinol.* **118,** 218–226 (1988).
38. Generoso, W. M., Stout, S. K. & Huff, S. W. Effects of alkylating agents on reproductive capacity of adult female mice. *Mutat. Res.* **13,** 171–184 (1971).
39. Shiromizu, K., Thorgeirsson, S. S. & Mattison, D. R. Effect of cyclophosphamide on oocyte and follicle number in Sprague–Dawley rats, C57BL/6N and DBA/2N mice. *Pediatr. Pharmacol.* **4,** 213–221 (1984).
40. Hadjantonakis, A. K., Gertsenstein, M., Ikawa, M., Okabe, M. & Nagy, A. Generating green fluorescent mice by germline transmission of green fluorescent ES cells. *Mech. Dev.* **76,** 79–90 (1998).
41. Nagano, M. C. Homing efficiency and proliferation kinetics of male germ line stem cells following transplantation in mice. *Biol. Reprod.* **69,** 701–707 (2003).
42. Szilvassy, S. J., Ragland, P. L., Miller, C. L. & Eaves, C. J. The marrow homing efficiency of murine hematopoietic stem cells remains constant during ontogeny. *Exp. Hematol.* **31,** 331–338 (2003).
43. Torrente, Y. *et al.* Identification of a putative pathway for the muscle homing of stem cells in a muscular dystrophy model. *J. Cell Biol.* **162,** 511–520 (2003).
44. Oh, H. *et al.* Cardiac progenitor cells from adult myocardium: homing, differentiation, and fusion after infarction. *Proc. Natl Acad. Sci. USA* **100,** 12313–12318 (2003).
45. Pearl, R. & Schoppe, W. F. Studies on the physiology of reproduction in the domestic fowl. *J. Exp. Zool.* **34,** 101–118 (1921).
46. Tilly, J. L. Ovarian follicle counts—not as simple as 1, 2, 3. *Reprod. Biol. Endocrinol.* **1,** 11 (2003).
47. Walpita, D., Plug, A. W., Neff, N. F., German, J. & Ashley, T. Bloom's syndrome protein, BLM, colocalizes with replication protein A in meiotic prophase nuclei of mammalian spermatocytes. *Proc. Natl Acad. Sci. USA* **96,** 5622–5627 (1999).
48. Russell, L. B., Hunsicker, P. R., Hack, A. M. & Ashley, T. Effect of the topoisomerase-II inhibitor etoposide on meiotic recombination in male mice. *Mutat. Res.* **464,** 201–212 (2000).
49. Foley, J. G. D. & Bard, J. B. L. Apoptosis in the cortex of the developing mouse kidney. *J. Anat.* **201,** 477–484 (2002).
50. Walter, I. *et al.* Rapid and sensitive detection of enhanced green fluorescent protein expression in paraffin sections by confocal laser scanning microscopy. *Histochem. J.* **32,** 99–103 (2000).

Supplementary Information accompanies the paper on **www.nature.com/nature**.

Acknowledgements We thank Y. Morita for technical assistance; T. Noce for MVH antiserum; T. Ashley for SCP3 antiserum; and I. Schiff and F. Frigoletto Jr for critical reading of the manuscript before its submission. This work was supported by the National Institute on Aging and by Vincent Memorial Research Funds. This study was conducted while J.L.T. was an Investigator of the Steven and Michele Kirsch Foundation, and while J.J. was a Research Fellow supported by The Lalor Foundation.

Competing interests statement The authors declare that they have no competing financial interests.

Correspondence and requests for materials should be addressed to J.L.T. (jtilly@partners.org).

picosecond absorption spectroscopy. *Photosyn. Res.* **22,** 211–217 (1989).
15. Beekman, L. M. *et al.* Trapping kinetics in mutants of the photosynthetic purple bacterium *Rhodobacter sphaeroides*: influence of the charge separation rate and consequences for the rate-limiting step in the light-harvesting process. *Biochemistry* **33,** 3143–3147 (1994).
16. Frese, R. N. *et al.* The long-range supraorganization of the bacterial photosynthetic unit: A key role for PufX. *Proc. Natl Acad. Sci. USA* **97,** 5197–5202 (2000).
17. Scheuring, S. *et al.* Nanodissection and high-resolution imaging of the *Rhodopseudomonas viridis* photosynthetic core complex in native membranes by AFM. *Proc. Natl Acad. Sci. USA* **100,** 1690–1693 (2003).
18. Hess, S. *et al.* Temporally and spectrally resolved subpicosecond energy transfer within the peripheral antenna complex (LH2) and from LH2 to the core antenna complex in photosynthetic purple bacteria. *Proc. Natl Acad. Sci. USA* **92,** 12333–12337 (1995).
19. Scheuring, S. *et al.* AFM characterization of tilt and intrinsic flexibility of *Rhodobacter sphaeroides* light harvesting complex 2 (LH2). *J. Mol. Biol.* **325,** 569–580 (2003).
20. Katona, G., Andreasson, U., Landau, E. M., Andreasson, L. E. & Neutze, R. Lipidic cubic phase crystal structure of the photosynthetic reaction centre from *Rhodobacter sphaeroides* at 2.35 angstrom resolution. *J. Mol. Biol.* **331,** 681–692 (2003).
21. Scheuring, S. *et al.* Structural role of PufX in the dimerization of the photosynthetic core-complex of *Rhodobacter sphaeroides*. *J. Biol. Chem.* **279,** 3620–3626 (2004).
22. Sturgis, J. N. & Niederman, R. A. The effect of different levels of the B800–850 light-harvesting complex on intracytoplasmic membrane development in *Rhodobacter sphaeroides*. *Arch. Microbiol.* **165,** 235–242 (1996).
23. Müller, D. J. *et al.* Observing membrane protein diffusion at subnanometer resolution. *J. Mol. Biol.* **327,** 925–930 (2003).
24. Berry, E. A. *et al.* X-ray structure of *Rhodobacter capsulatus* cytochrome bc_1: Comparison with its mitochondrial and chloroplast counterparts. *Photosyn. Res.* (in the press).
25. Feniouk, B. A., Cherepanov, D. A., Voskoboynikova, N. E., Mulkidjanian, A. Y. & Junge, W. Chromatophore vesicles of *Rhodobacter capsulatus* contain on average one F_oF_1-ATP synthase each. *Biophys. J.* **82,** 1115–1122 (2002).
26. Boekema, E. J., van Breemen, J. F., van Roon, H. & Dekker, J. P. Arrangement of photosystem II supercomplexes in crystalline macrodomains within the thylakoid membrane of green plant chloroplasts. *J. Mol. Biol.* **301,** 1123–1133 (2000).
27. Niederman, R. A., Mallon, D. E. & Parks, L. C. Membranes of *Rhodopseudomonas sphaeroides*. VI. Isolation of a fraction enriched in newly synthesized bacteriochlorophyll α-protein complexes. *Biochim. Biophys. Acta* **555,** 210–220 (1979).
28. Van der Werf, K. O. *et al.* Compact stand-alone atomic force microscope. *Rev. Sci. Instrum.* **64,** 2892–2897 (1993).

Supplementary Information accompanies the paper on **www.nature.com/nature**.

Acknowledgements This work was supported by grants from the BBSRC (UK) and the Netherlands Organisation for Scientific Research (NWO). This paper is dedicated to the memory of Prof. Dr. Bart de Grooth.

Competing interests statement The authors declare that they have no competing financial interests.

Correspondence and requests for materials should be addressed to C.N.H. (c.n.hunter@shef.ac.uk).

corrigendum

Germline stem cells and follicular renewal in the postnatal mammalian ovary

Joshua Johnson, Jacqueline Canning, Tomoko Kaneko, James K. Pru & Jonathan L. Tilly

Nature **428,** 145–150 (2004).

In this Article, we estimated that germline stem cells generate approximately 77 new primordial oocytes per day in ovaries of postnatal female mice. It has since been drawn to our attention by Ton Schumacher that a line of reasoning used in our study to verify this value is circular. However, the initial value for daily oocyte renewal obtained from mathematical modelling is not derived from a circular argument. Accordingly, this oversight does not alter any of the data or the conclusions in our paper. □